# Back-propagation based beamformer design for Transverse Oscillations in Echocardiography

Xinxin Guo, Denis Friboulet, Hervé Liebgott

ACOUSTICS 2012

# Back-propagation based beamformer design for Transverse Oscillations in Echocardiography

X. Guo, D. Friboulet and H. Liebgott

Centre de recherche en applications et traitement de l'image pour la santé, 7 avenue Jean Capelle, Bat Blaise Pascal, 69621 Villeurbanne Cedex
xinxin.guo@creatis.insa-lyon.fr

Abstract— Transverse oscillation (TO) imaging is a technique that produces ultrasound radiofrequency images featuring oscillations in both spatial dimensions. This is natural for axial direction but necessitates specific beamforming for transverse direction. Conventional TO beamformer design using Fraunhofer approximation has been properly developed in linear geometry. Using cosine function modulated by Gaussian as a lateral profile, the apodization function defined as inverse Fourier transform of the profile thus corresponds to the convolution between a Gaussian and two Dirac. This approach works well in linear geometry but is limited for sector scan as in echocardiography. We propose to use back-propagation based on reciprocity theorem, which appropriately takes into account the fact that the expected oscillation profiles are in polar coordinate. To validate with simulations using Filled II, the comparison of PSFs obtained using FA and back-propagation with theoretical profiles is quantified using root mean square error. The result clearly shows that PSFs obtained using back-propagation are more accurate than using FA. But it has declining advantages than FA at larger depth because the transformation from Cartesian to polar coordinate becomes closer for FA. The next step is to validate that the obtained PSF and associated TO allow more accurate motion estimates.

# 1 Introduction

Nowadays, clinical diagnosis is greatly depending on medical imaging. It motivates many groups work on improving images qualities, or motion estimation accuracy in other words. Ultrasound imaging is a widely used imaging modality with applications such as echocardiography, blood flow and elastography; as it permits to acquire real-time images to present the acoustic properties of studied tissues thanks to its high frame-rate capacity. Compared with other imaging modalities such as MRI or X-ray, echography possesses advantages of non-invasive, non-ionizing to patients and low cost in diagnosing. In cardiac imaging, conventional echocardiography is however facing some difficulties to estimate the motion of the heart with high accuracy in the transverse direction (the direction perpendicular to the beam axis). Working on the image formation, this problem can be addressed by modifying the beamforming scheme in order to introduce transverse oscillations (TO) in the system point spread function (PSF).

Presently, three groups are mainly taking TO as means of beamforming design for image formation. It was firstly raised by Jensen and al. [1] and Anderson [2] in the field of blood flow. It has potential to be applied in clinical applications because it has been tested in vivo as presented in [3] and [4]. In the field of elastography, Sumi proposed to use a lateral modulation method [5, 6] to achieve a high measurement accuracy. Our group implants TO both in elastography [7, 8] and echocardiography [9, 10], and obtained encouraging experimental results based on different beamforming strategies and estimators.

The improvement for motion estimation using TO in these studies has been presented in linear geometry. Classical beamforming design uses Fraunhofer approximation to achieve the formation of TO featured images in linear geometry. This approximation shows an acknowledge that the apodization function and the system PSF can relate to each other through a simple Fourier transform. In view of the merits in application of TO in linear geometry, we take the challenge of adapting this technique for sectorial scans. However, the conventional Fraunhofer-based beamforming cannot yield satisfactory TO patterns in our preliminary investigations [9]. Therefore in this paper we propose a new back-propagation based beamformer design for transverse oscillations in echocardiography.

The paper is organized as follows: in section II we briefly recall the principle of obtaining TO images in linear geometry using Fraunhofer approximation and give the transform from linear to sectorial geometry, the principle of BP and its application in sector scan; section III provides the evaluation of the accuracy of proposed BP method, and a comparison with conventional beamforming; section IV is the discussion and in section V we give the conclusion.

# 2 Principle of transverse oscillations and back-propagation

The accuracy of motion estimation can be respectively affected by either the estimator or the beamformer design. The latter factor mainly effects the formation of TO images, which enables to control the shape of the PSF. This control can be realized through a specific beamforming scheme, i.e. specific time delay and apodization functions that are imposed to different emitting signals. Our interest is mainly focused on the acquisition of apodization function by means of expected PSFs. In this section, the methodology of how to design the beamformer parameters using conventional Fraunhofer approximation to obtain TO images is presented and then the proposed back-propagation method is explained in detail.

## 2.1 Principle of transverse oscillations using Fraunhofer approximation

*Fraunhofer approximation for linear geometry*

As in conventional beamforming, the lateral PSF profile cannot show the satisfied oscillations as those naturally present in the axial direction. Committed to achieve better lateral oscillations in a linear geometry setting, such a lateral profile [11] can be expressed in eq. (1), which is a multiplication of a Gaussian envelope with a cosine function. In this equation, $\lambda_x$ is the expected lateral wavelength, $\sigma_x$ is the half maximum width of the Gaussian envelop, and $u_x = 1/\lambda_x$ .

$$h(x) = \cos(2\pi u_x) \cdot \exp(-\pi(\frac{x}{\sigma_x})^2) . \quad (1)$$

The beamforming that we do to obtain the profile expressed in eq. (1) is classically based on Fraunhofer approximation, the conditions of which are met at the focal point. In order to be able to apply the Fraunhofer approximation along the whole propagation path, the delay function is set so as to perform dynamic quadratic focusing. Under this approximation, the transverse profile of the PSF at the depth of focusing is related to the apodization function by a Fourier transform[12]. In line with this

theory, as be transformed by inverse Fourier transform of PSF profile with TO in eq. (1), the apodization function is clearly expressed as follows:

$$w_r(x) = \frac{1}{2}(\exp^{-\pi(\frac{x-x_0}{\sigma_0})^2} + \exp^{-\pi(\frac{x+x_0}{\sigma_0})^2}) . \quad (2)$$

Where $x_0 = \lambda y/\lambda_x$ and $\sigma_0 = \sqrt{2}\,\lambda y/\sigma_x$ , $\lambda$ is the wavelength of the transmitted pulsed, y is the depth of interest, $\pm x_0$ is the position of the two peaks and $\sigma_0$ is the half maximum width of each peak. The lateral PSF profile in eq. (1) and the apodization function (2) are represented in Figure 1.

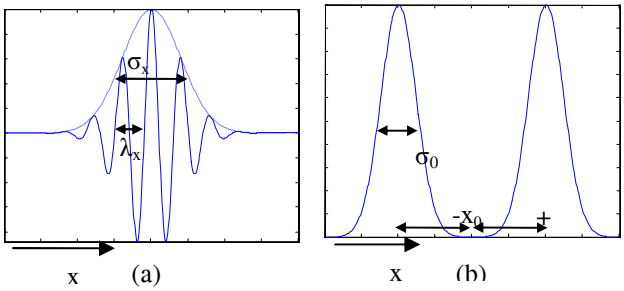


Figure 1: Representation of the lateral PSF profile (a) and the corresponding apodization function in (b).

***Fraunhofer approximation for sectorial geometry***

As the framework that has been introduced above is derived for linear geometry, when considering adapting it to sectorial geometry, transforming the model parameters from Cartesian coordinates to polar coordinates is necessary. This is done by setting (see Figure **2**): $\lambda_x \approx \lambda_\theta \cdot r$ , $\sigma_x = \sigma_\theta \cdot r$ , and $y \approx r$ , where $\lambda_\theta$ is the expected lateral wavelength of PSF profile in radians, $\sigma_\theta$ is the standard deviation of PSF profile, and $r$ is the sweeping radius. Based on the approximation settings above, the position of two peaks $\pm x_{\theta 0}$ and the standard deviation $\sigma_{\theta 0}$ of the apodization function are given as follows:

$$x_{\theta 0} \approx \lambda/\lambda_\theta . \quad (3)$$

$$\sigma_{\theta 0} \approx \sqrt{2}\lambda/\sigma_\theta . \quad (4)$$

Eq. (3) and (4) show an interesting result that $x_{\theta 0}$ and $\sigma_{\theta 0}$ are independent from depth which is different from the case as in linear geometry, but only be limited to the values of the lateral wavelength and the half maximum width of the Gaussian envelop in angles.

## 2.2 Principle of back-propagation

***Back-propagation for linear geometry***

As Fraunhofer approximation is obtained under the assumption that the inverse Fourier Transform of PSF profile is an approximation of the apodization function, the obtained TO images does not precisely along the shape of expected profiles. The limitation of Fraunhofer approximation drives us to propose a new TO beamformer design using BP which can provide more accurate images.

The PSF pressure field at the focus can be considered as a combined effect of ultrasound signals sent by all the aperture elements. For ultrasound signals, the Green function is considered as the ultrasound propagation function from the i[th] element to a point of interest [12]. In a linear geometry setting, under this case, the pressure p(x,y) at the depth y and lateral position x is equal to

$$p(x,y) = \sum_{i=1}^{N} w(x_i)\frac{e^{\frac{j2\pi r_i}{\lambda}}}{r_i} . \quad (5)$$

Where N is the number of active elements, $x_i$ is the position of ith element, $r_i$ is the distance from the i[th] element to the point of interest.

Under reciprocity theorem, the apodization function in eq. (5) can be considered as the pressure that would be observed at the position of aperture elements where now is regarded as the depth of interest and the actual apodized function is in revenge the pressure profile p(x,y). This approach is thus called BP of the pressure field towards the aperture and can be expressed as

$$w_r(x_i, y_0) = \int_{-\infty}^{+\infty} p(x, y_0)\frac{e^{\frac{j2\pi r_{i0}}{\lambda}}}{r_{i0}}dx . \quad (6)$$

Where $y_0$ is the depth of interest, $p(x, y_0)$ is the pressure profile at the depth of interest, $r_{i0}$ is the distance from i[th] element to the point of interest.

***Back-propagation for sectorial geometry***

In linear geometry configuration, the expected PSF profile is a function with lateral positions as variables at the same level of depth, origin from the same principle, the profile in sector scan is set as a function of angles but is a copy from one level of radius to another. The sectorial configuration is vividly presented in Figure 2.

Figure 2(a) and (b) correspond to different situations when the beam sweeps in the direction $\theta_1$ and $\theta_2$ respectively. Θ is the angle of scan area, $r_0$ is the scan radius. Apodization functions which are presented as $w_{r1}(x, r_0)$ and $w_{r2}(x, r_0)$ corresponding to expected profiles of $p(\theta_1, r_0)$ and $p(\theta_2, r_0)$ respectively.

The basic idea of BP expressed in Fig 2 could be explained as follows: in the area of interest indicated as Θ the beam sweeps from one side to another as a function of time to detect the scatters. Owing to unknownness of the positions of scatters, we assumed to obtain the same shaped PSF profile in each direction, as be indicated in figure 2 (a) and (b) which take the directions of $\theta_1$ and $\theta_2$ for example. Under this assumption, the beamforming can appropriately adapt to sector since the apodization function brings into correspondence with the PSF profile. Derived from eq. (6) to polar coordinates, the apodization function adapted to sectorial geometry can be expressed as in eq. (7).

$$w_r(x_i, r_0) = \int_{-\frac{\Theta}{2}}^{\frac{\Theta}{2}} p(\theta, r_0) \frac{e^{\frac{j2\pi r_{i0}}{\lambda}}}{r_{i0}} d\theta \,. \quad (7)$$

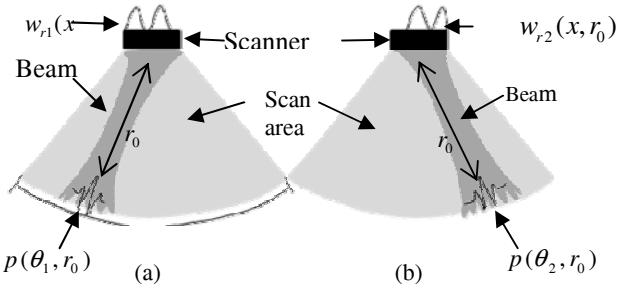


Figure 2: Presentation of sector scan using back-propagation with transverse oscillations. Θ is the angle of scan area, $\theta_1$ and $\theta_2$ are the different scan directions, $r_0$ is the scan radius. Apodization functions which are presented as $w_{r1}(x, r_0)$ and $w_{r2}(x, r_0)$ corresponding to expected profiles of $p(\theta_1, r_0)$ and $p(\theta_2, r_0)$ respectively.

# 3 Simulations and results

Numerical simulations are performed using the software Field II [13, 14]. For computer simulations, the parameter values were chosen so that they correspond to a possible future experimental ultrasound image formation. We use a linear array probe with 64 elements to do sector scan. The basic parameters used in our simulations are presented in Table 1.

Table1: simulation parameters used in Field II and parameters used in emission.

| Parameter | Value |
|---|---|
| Center frequency | 3MHz |
| Sampling frequency | 100MHz |
| Element height | 5mm |
| Elements width | λ/2 |
| Distance between 2 elements | 0.1mm |
| Focus in emit | Plane wave |
| Apodization in emit | Hanning |
| Lateral wavelength in angles | $\lambda_\theta = 4°$ |
| Standard deviation of PSF profile | $\sigma_\theta = 1.5\lambda_\theta$ |

The methodology that we use to evaluate the accuracy is by comparing the expected, theoretical point spread function $PSF^{th}$, and the PSF obtained in the simulation by applying a beamforming/ apodization scheme, noted $PSF^{real}$. $PSF^{real}$ is obtained by applying either the proposed BP approach or the conventional Fourier based technique in simulations. The measure used in simulations to quantify the accuracy of estimation is by taking the root mean square error (RMSE) as defined in eq. (8). Calling $PSF_i^{th}$ the ith value of the theoretical expected PSF and $PSF_i^{real}$ the ith PSF value obtained in simulations using Fourier relation or BP, N is equal to the number of lines of image, the RMSE is given as in eq.(8).

$$RMSE = \sqrt{\frac{1}{N}\sum_i^N (PSF_i^{th} - PSF_i^{\exp})^2} \,. \quad (8)$$

In simulations, the scatters were set in the front and on the side of aperture as well as in different depths, in order to observe the performance of our proposed BP method comprehensively. We will pay specific attention on the side of the sector as it corresponds to the place where the most important error will be observed. At the same time, it is also an indicator of the adaptive performance of our method.

Figure 3 (b) gives a presentation of apodization function obtained in the area from -45° to 45° for sector scan. More in detail, Figure 3(a) shows a comparison of apodization functions obtained using Fourier relation and BP in the direction of 0°. Furthermore, the apodization functions obtained from all different angles in scan area using BP method are presented in Fig. 3(b) and **(c)** is the presentation of apodization functions corresponding to directions 30 and -30°, as indicated in Fig. 3(b).

The two profiles of apodization function in Fig 3(a) are different to each other but they are symmetry to the centeral element respectively. Fig. 3(b) shows that the apodization functions are slightly asymmetric with respect to the central element in corresponding with different directions. This can be better seen from Fig. 3(c) which shows the apodization profile for directions -30° and 30°.

We use the apodization functions presented in Fig.3 to get PSF images. In order to observe the performance of these methods, we give a comparison of expected PSF profiles obtained using Fourier relation and the proposed BP method in Fig. 4 for different depths of 60mm and 70mm in the direction of 0°, and moreover in the direction of 30° at the depth of 60mm. Then the accuracy measure of RMSE is taken to calculate the precision of estimated profiles.

For the purpose of clearly distinguishing different profiles in Fig. 4, the BP-based profiles are in dotted red lines and Fourier-based profiles in solid blue lines, the expected theoretical profiles are given in solid black lines.

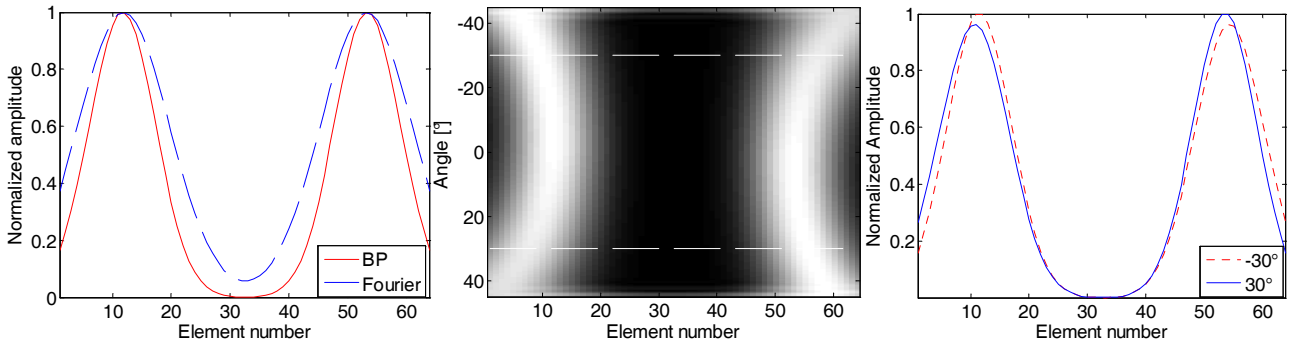


Figure 3:Presentation of apodization functions for sector scan: (a) presents apodized profiles using Fourier relation in dotted line and back-propagation in solid line in 0°; (b) is apodization function of BP for all sweeping angles; (c) gives the indicated apodization for directions 30 and -30°, corresponding to the two dotted lines in (b).

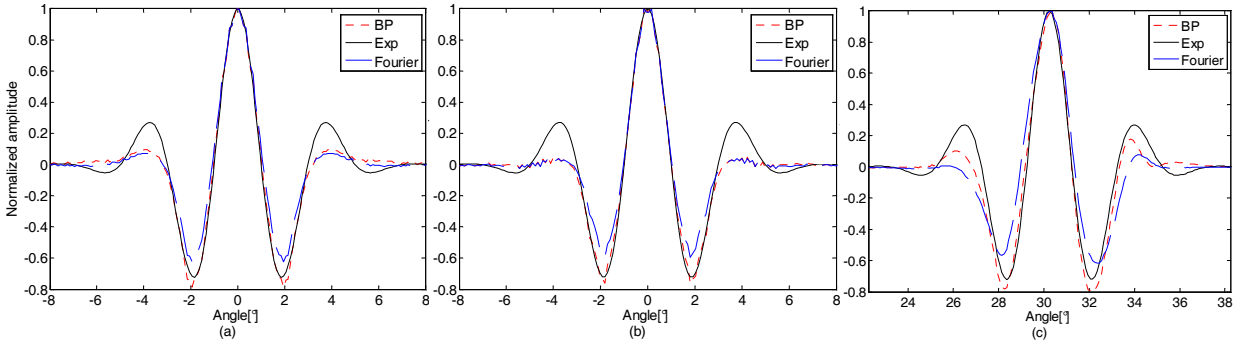


Figure 4: PSF profiles obtained in direction of 0° at different depth: 60 mm in (a) and 70 mm in (b). (c) presents the PSF profiles obtained in the direction of 30° at a depth of 60 mm. The profiles in dotted lines are obtained using Fourier relation, BP in dashed lines and expected profiles in solid lines.

# 4 Discussion

The profiles obtained using BP method and Fourier relation in the direction of 0° at the depth of 60mm compared with the expected profile are presented in Fig. 4(a) It may be observed that the profiles corresponding to BP are slightly closer to the expected ones as compared to the profiles associated to Fourier-based beamforming. This is confirmed by the RMSE which is equal to $3.86 \times 10^{-2}$ for the Fourier-based profiles and which is $3.04 \times 10^{-2}$ for the BP-based profiles in Fig. 4(a), which indicates that BP-based method brings an improvement of 21%.

Profiles obtained in the same direction than (a) but with a depth are of 70 mm presented in Fig 4(b) and yields the same conclusion: the profile associated to BP leads the same accuracy than the Fourier- based profile, with a RMSE equal to $3.62 \times 10^{-2}$ for BP and $4.26 \times 10^{-2}$ for Fourier-based beamforming, which also brings an improvement of 15% when compare with the Fourier-based profile. Here the improvement is smaller as radian changes slightly at larger depth, thus the approximation expressed in eq. (3)-(4) brings little and little error with deeper depth when using Fraunhofer approximation. It changes when observing the results obtained for direction far from the probe axis.

Fig.4(c) shows the results obtained for a direction of 30° away from this axis. It also presents an improvement brought by BP over Fourier-based beamforming, which is confirmed by the RMSE which is equal to $6.46 \times 10^{-2}$ for the Fourier-based profile and $3.59 \times 10^{-2}$ for the BP-based, not difficult to see that our proposed method brings almost an improvement of 50%.

The difference between obtained profiles and expected PSFs is resulting from several aspects: the approximate transformation from $x_0$ and $\sigma_0$ in Cartesian coordinates to $x_{\theta 0}$ and $\sigma_{\theta 0}$ in polar coordinates, which can be seen at the end of subsection of 2.1; the dimension of element is not negligible, yielding approximation error when the distance from the element to the point of interest is calculated; another factor is that the Green function used as the propagation function in eq. (5) is monochromatic whereas ultrasound image is obtained using broadband signals.

As in the case of the Fraunhofer approximation, using the proposed BP method the apodization function keeps also constant even if the depth changes in sector scan, as shown by eq. (3)-(4). As a result, in simulations, the same apodization function can be imposed to all signals received from the same direction, by this means, the time cost of calculation could be greatly reduced, it is of great importance in research.

Figure 5 is obtained with the same PSF profile in the direction of 0° but with different element numbers from Fig. 3(a). Compared with Fig. 3(a) which is obtained with 64 elements, we can see that the apodization function is not as complete as obtained with 128 elements. It will bring about some error in image formation. What's more, in order to improve the estimation accuracy one might be interested in decreasing the value of the lateral PSF wavelength. This would need larger probes, which is unfortunately not possible due to the acquisition that has to be done between the ribs for echocardiography. The quality of the estimation result might be improved with larger probes performing a sectorial scan for other medical applications.

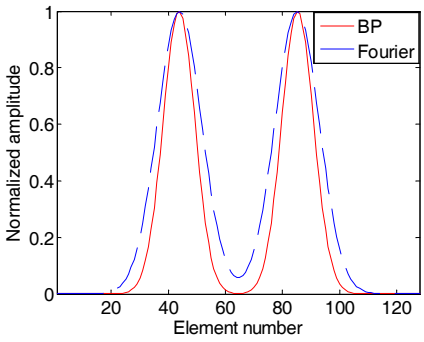


(a)

Figure 5: Apodization function profiles obtained using back-propagation in solid line and Fourier relation in dotted line with elements number = 128. Parameters are $\lambda_\theta = 4°$ and $\sigma_\theta = 1.5 * \lambda_\theta$

# 5 Conclusion

In this paper, our methodology of transverse oscillations beamformer design using back-propagation has been introduced.

Firstly we introduce the principle of transverse oscillations obtained with Fraunhofer approximation both in linear and sector geometry, and explained in detail the evolvement from linear and sector configuration for proposed back-propagation method.

Secondly, with specify value of parameters, we use the apodization functions obtained using back-propagation and Fourier relation in different directions to get PSF images with scatters located at different depths and different directions in simulation. Under the accuracy measure of RMSE, we can get a conclusion that the proposed back-propagation method brings some improvements than the conventional Fraunhofer approximation

Although the improvement of our method has been observed when compared to Fourier relation, further confirmation need to be done by using experimental acquisitions. The potential for diagnosing diseases can be evaluated in further studies.

# Acknowledgments

This work has been partially supported by Centre Lyonnais d'Acoustique (CeLyA), ANR grant n°2011-LABX-014 and by ANR JCJC grant US-Tagging.

# References

[1] J. A. Jensen and P. Munk, "A new method for estimation of velocity vectors," *Ultrasonics, Ferroelectrics and Frequency Control, IEEE Transactions on,* vol. 45, pp. 837-851, 1998.

[2] M. E. Aderson, "Multi-dimensional velocity estimation with ultrasound using spatial quadrature," *Ultrasonics, Ferroelectrics and Frequency Control, IEEE Transactions on,* vol. 45, pp. 852-861, 1998.

[3] J. Udesen, M. B. Nielsen, K. R. Nielsen, and J. A. Jensen, "Examples of< i> In Vivo</i> Blood Vector Velocity Estimation," *Ultrasound in medicine & biology,* vol. 33, pp. 541-548, 2007.

[4] K. Hansen, J. Udesen, C. Thomsen, J. A. Jensen, and M. Nielsen, "In vivo validation of a blood vector velocity estimator with MR angiography," *Ultrasonics, Ferroelectrics and Frequency Control, IEEE Transactions on,* vol. 56, pp. 91-100, 2009.

[5] C. Sumi, "Multidimensional displacement vector measurement methods utilizing instantaneous phase," 2005, pp. 1704-1707.

[6] C. Sumi, "Displacement vector measurement using instantaneous ultrasound signal phase-multidimensional autocorrelation and Doppler methods," *Ultrasonics, Ferroelectrics and Frequency Control, IEEE Transactions on,* vol. 55, pp. 24-43, 2008.

[7] H. Liebgott, J. Fromageau, J. E. Wilhjelm, D. Vray, and P. Delachartre, "Beamforming scheme for 2D displacement estimation in ultrasound imaging," *EURASIP journal on applied signal processing,* vol. 2005, pp. 1212-1220, 2005.

[8] H. Liebgott, J. E. Wilhjehm, J. A. Jensen, D. Vray, and P. Delachartre, "PSF dedicated to estimation of displacement vectors for tissue elasticity imaging with ultrasound," *Ultrasonics, Ferroelectrics and Frequency Control, IEEE Transactions on,* vol. 54, pp. 746-756, 2007.

[9] H. Liebgott, A. Basarab, S. Marincas, O. Bernard, and D. Friboulet, "Tangential oscillations for motion estimation in echocardiography," 2008, pp. 1761-1764.

[10] H. Liebgott, A. Ben Salem, A. Basarab, H. Gao, P. Claus, J. D'Hooge, P. Delachartre, and D. Friboulet, "Tangential sound field oscillations for 2D motion estimation in echocardiography," 2009, pp. 498-501.

[11] H. Liebgott, "Impulse response synthesis in ultrasound imaging for vectorial displacement estimation", Ph.D. thesis, 2005.

[12] J. W. Goodman, *Introduction to Fourier optics*: Roberts & Company Publishers, 2005.

[13] J. A. Jensen, "Field: A program for simulating ultrasound systems," 1996.

[14] J. A. Jensen and N. B. Svendsen, "Calculation of pressure fields from arbitrarily shaped, apodized, and excited ultrasound transducers," *Ultrasonics, Ferroelectrics and Frequency Control, IEEE Transactions on,* vol. 39, pp. 262-267, 1992.